



PRESSURE GRADIENT PREDICTION FOR DIFFERENT FLOW PATTERNS OF HEAVY OIL AND NATURAL GAS IN A HORIZONTAL PIPE USING CFD TECHNIQUES AND EMPIRICAL CORRELATIONS

^a Silva, L. D. S. ¹; ^b Marinho, J. L. G.; ^b Oliveira, L. M. T. M.

^a Department of Chemical Engineering, Federal University of Alagoas, Maceió – AL, Brazil

^b Department of Petroleum Engineering, Federal University of Alagoas, Maceió – AL, Brazil

Received: 01.08.2017 / Revised: 05.10.2017 / Accepted: 05.10.2017 / Published on line: 16.10.2017

ABSTRACT

Two-phase flows are of fundamental importance in the petroleum industry, considering that most petroleum reservoirs produce oil and gas simultaneously. Because system pressure gradient is a result of the frictional effects between fluids and pipe wall, and the interfacial effects between the fluids themselves, the precise determination of this parameter is complex. Many authors have sought to predict pressure gradient by using computational fluid dynamic techniques and empirical correlations. The present work aims to compare heavy oil and natural gas mixture pressure gradients in a horizontal pipe for different flow patterns using the application ANSYS CFX 13.0, Lockhart and Martinelli, and Beggs and Brill correlations. The analysis investigated the results for bubbly, plug, and stratified flows. The results showed that Beggs and Brill over predicted pressure gradient values. It was also observed a good agreement between numerical and Lockhart and Martinelli correlation for bubbly and plug flows, with root-mean-square deviations (RMSD) of 5.78 and 19.55 percent, respectively. As for the stratified flow cases, the numerical results presented a poor agreement, with a RMSD greater than 90 percent. The high percent deviation for this flow regime is due to the increase in the gas input content. To compute the high gas velocity effects and, hence, improve the agreement, we suggest the use of turbulence and free surface models as well as different values of drag coefficient in the numerical setup.

KEYWORDS

pressure gradient; CFX; flow patterns; Lockhart and Martinelli correlation; Beggs and Brill correlation

¹ To whom all correspondence should be addressed.

Address: Department of Chemical Engineering, Federal University of Alagoas, Ave. Lourival Melo Mota, s/n Tabuleiro, Maceió – AL – Brazil.

ZIP Code: 57072-970 | Phone: +55 82 99600-3504 | e-mail: lucasdavid.eq@gmail.com

doi:10.5419/bjpg2017-0015

1. INTRODUCTION

Many authors have studied two-phase flow systems due to their importance in several industrial processes (Foletti et al., 2011). Since most reservoirs produce oil and gas simultaneously, the two-phase flow also occurs in the petroleum transport (Thomas et al., 2001). Because of the presence of a liquid-gas interface in these systems, since more energy is dissipated due to frictional effects, there is an increase in pressure gradient and also in the energy required to pump the oil and gas mixture (Coates & Pressburg, 1959).

Depending on fluid properties, such as density, viscosity, and interfacial tension, the liquid-gas interface may present different flow pattern configurations (Angeli & Hewitt, 2000). Pipe inclination and flow operational conditions are also parameters that can affect the flow regime. Because design parameters, such as pressure gradient, depend strongly on flow pattern, the determination of the latter is crucial for a reliable pumping system design (Matsubara & Naito, 2011).

In the last years, one could observe the development of several empirical maps to predict two-phase flow patterns. Low-viscosity fluids such as water and air are the most common fluids used in test facilities to build those maps. Despite the good agreement between empirical data and the experimental results in air-water systems, empirical maps at times have failed to predict flow patterns satisfactorily for systems with high-viscosity fluids such as heavy oil and gas (Foletti et al., 2011). To account the properties of the fluids, one may use the flow map developed by Baker (1954), in which the flow pattern is a function of non-dimensional parameters.

The pressure gradient must also be determined precisely to design liquid-gas flow systems properly. Lockhart and Martinelli correlation is used widely to predict pressure gradient in gas-liquid flow systems. The experimental facility from which the correlation was developed consisted of 0.00149-m and 0.0258-m inner diameter sections of horizontal pipes. The authors used data for simultaneous flow of air with water, benzene, kerosene, and various oils to develop the correlation (Cui & Chen, 2010). Because of its simplicity and accurate predictions, the Lockhart

and Martinelli correlation was included in this study.

Beggs and Brill correlation is also one of the many empirical models cited by several authors as a classic correlation since it works for any pipe inclination and flow pattern (Sarah et al., 2014; Souza et al., 2010). The authors used a small facility consisting of 0.0254-m and 0.0381-m sections of a 27.43-m long acrylic pipe with inclination angle range of variation of -90° to $+90^\circ$. Even though Beggs and Brill developed this correlation originally for water-air flow systems, it has been used extensively in oil-gas two-phase flows due to its reliable predictions (Beggs & Brill, 1991; Sarah et al., 2014; Souza et al., 2010; Zhao et al., 2013).

One can also gain an understanding of the two-phase flow phenomena with the aid of Computational Fluid Dynamics techniques (CFD), which uses a mathematical model based on conservation of mass, momentum, and energy. Commonly, numerical methods are more advantageous over the analytical and experimental methods since they can be obtained quickly and at a lower cost. Nevertheless, experimental validation is required to confirm their reliability (Silva & Marinho, 2016; Souza et al., 2011).

The present work aims to compare heavy oil and natural gas mixture pressure gradients in a horizontal pipe for different flow patterns. The application Ansys CFX 13.0 was used to obtain the pressure gradient for the bubbly, plug, and stratified flow regimes. Following, the results were compared with those predicted by Lockhart and Martinelli, and Beggs and Brill correlations.

2. METHODOLOGY

To perform the present work, the study was divided in the following major steps:

- Definition of the physical problem;
- Determination of the flow pattern;
- Mathematical formulation for the simulations on Ansys CFX 13.0;
- Mathematical formulation of Lockhart and Martinelli correlation;

- Mathematical formulation of Beggs and Brill correlations.

2.1 Physical problem description

The proposed domain consists of a 1-m segment length of a representative horizontal pipe with an inner diameter $D = 0.0254$ m. Due to the importance of this work for the petroleum industry, the duct is assumed as part of an oil production pipeline, as shown in Figure 1 in a simplified schematics.

2.2 Physical properties of the fluids

This study considered an isothermal flow at 298.15 K and an outlet pressure equal to $p = 101,325$ Pa. Although the pressure of the gas inside the pipe usually reaches larger values, the present study adopted the natural gas to be under atmospheric conditions. This simplification is due to the low gas flow rate, as presented in section 2.3, which allowed neglecting the compressible effects for the gas phase. Table 1 presents the physical properties of the fluids.

2.3 Flow pattern determination

The flow pattern was determined using the Baker's map, as shown in Figure 2. Equations 1 and 2 show the calculation of the non-dimensional parameters λ and ψ :

$$\lambda = \left(\frac{\rho_G \rho_L}{\rho_{air} \rho_{water}} \right)^{0.5} \quad (1)$$

$$\psi = \frac{\sigma_{water}}{\sigma} \left[\left(\frac{\mu_L}{\mu_{water}} \right) \left(\frac{\rho_{water}}{\rho_L} \right)^2 \right]^{1/3} \quad (2)$$

Where ρ_G , ρ_L , σ , and μ_L are density of the gas phase, density of the liquid phase, surface tension, and viscosity of the liquid phase, respectively. Reference properties are $\rho_{air} = 1.23$ kg/m³, $\rho_{water} =$

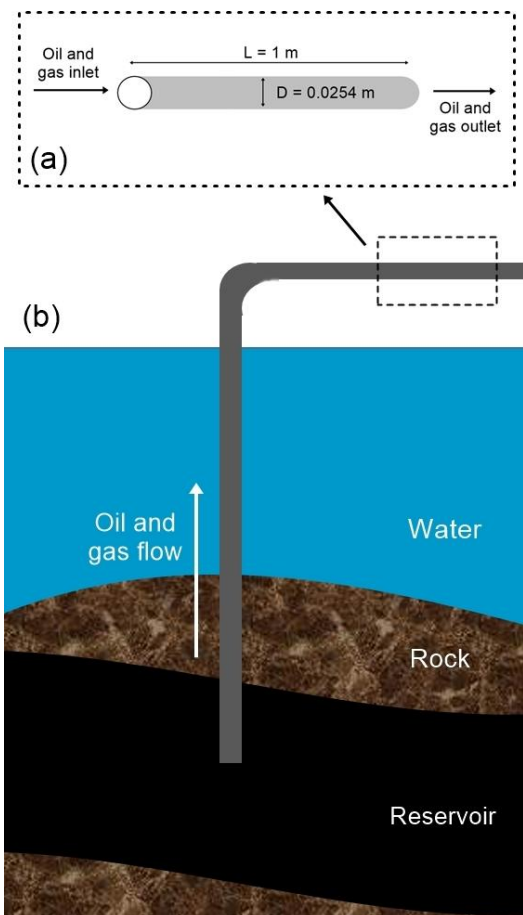


Figure 1. (a) Horizontal pipe and (b) Schematics of the oil formation and production pipeline.

1000 kg/m³, $\sigma_{water} = 0.072$ N/m, and $\mu_{water} = 0.001$ N.s/m² (Baker, 1954).

The mass fluxes m_L and m_G are functions of gas volume fraction r , mixture velocity v_m , and density of the fluids ρ_L and ρ_G (Equations 3 and 4):

$$m_L = (1 - r)v_m \rho_L \quad (3)$$

$$m_G = r v_m \rho_G \quad (4)$$

This study was limited to bubbly, plug, and stratified flow because they present low gas mass flow rates. This selection allowed some

Table 1. Physical properties of the fluids.

Fluid	μ (N.s/m ²)	ρ (kg/m ³)	Source
Natural gas	1.08E-5	0.7236	Silva and Marinho, 2014
Heavy oil	0.5	951	Barbosa et al., 2012

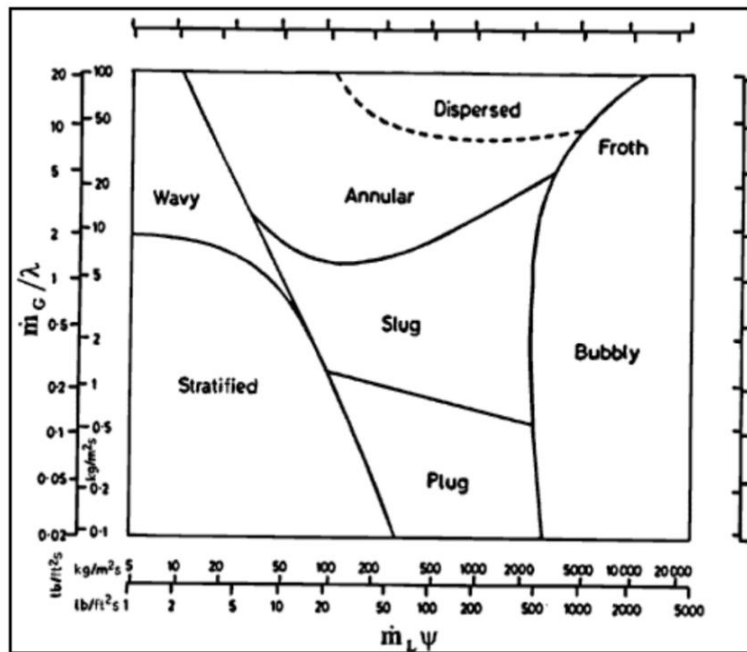


Figure 2. Baker's map for flow pattern prediction (Baker, 1954).

simplifications in the mathematical modeling such as incompressible flow and negligible non-drag forces.

Since λ and ψ depend only on the fluid properties, which, for our purposes, do not vary with the position, these parameters are constants. Therefore, the only variables of the Baker's map are the gas volume fraction r , and the mixture velocity v_m . To simplify, we fixed the latter at either 0.8 or 1.2 m/s, and selected values of r so that the (x, y) points in the Baker's map fall on the flow pattern regions. Table 2 presents the pairs of r and v_m for each regime.

2.4 Mesh generation and mathematical modeling on CFX

Since the CFD techniques are based on partial differential equations for the conservation of mass, momentum, and energy, the mesh generation is a necessary step to represent the domain in a simulation environment. Therefore, the pipe domain was divided into smaller control volumes with the aid of the application Ansys ICEM CFD. A mesh refinement test was performed to determine the optimum number of elements. Test results are presented in section 3.1. Figure 3 shows one of the meshes used in this test.

Table 2. Values of the gas volume fraction and the mixture velocity for different flow patterns.

Flow pattern	Case	r	v_m (m/s)	Case	r	v_m (m/s)
Bubbly flow	1	0.03	1.2	4	0.40	1.2
	2	0.20	1.2	5	0.50	0.8
	3	0.30	0.8	6	0.60	1.2
Plug flow	7	0.70	0.8	10	0.80	1.2
	8	0.75	0.8	11	0.85	0.8
	9	0.80	0.8	12	0.90	1.2
Stratified flow	13	0.97	0.8	16	0.97	1.2
	14	0.98	0.8	17	0.98	1.2
	15	0.99	0.8	18	0.99	1.2

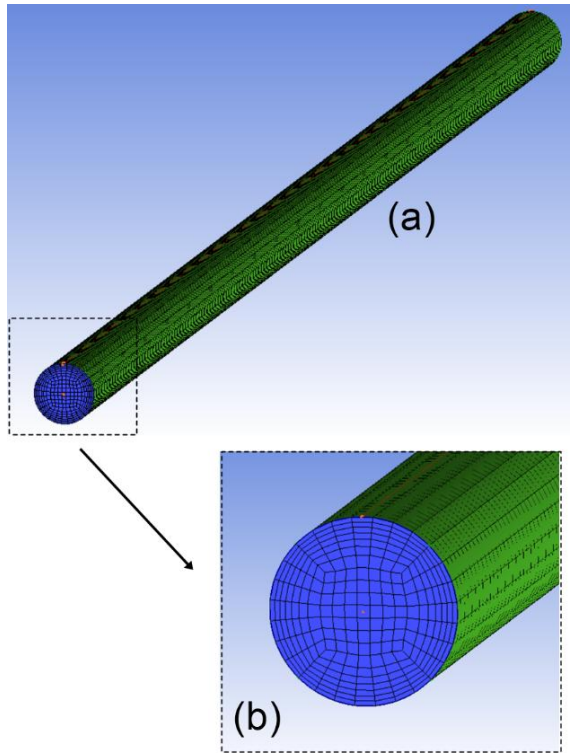


Figure 3. (a) Mesh used in the refinement test and (b) detail of the pipe inlet.

It is noteworthy that the volume of the elements closer to the wall were reduced (Figure 3(b)). Since the frictional effects and the velocity gradients are relevant in this region, the smaller elements therein will allow a better precision in the results.

To perform the simulations on Ansys CFX 13.0, the following assumptions were adopted:

- Isothermal flow;
- Smooth pipe;
- Gravitational effect;
- Tridimensional domain;
- Constant physical-chemical properties;
- Non-drag forces are negligible;
- No chemical reactions.

Since this work uses low gas flow rates, the problem may be simplified adopting incompressible flow. Tridimensional instabilities that continually occur in the two-phase flow were

also neglected so that a steady-state condition is valid. Based on these assumptions, Equations 5 and 6, which represent the mass and the momentum conservation, respectively, are the main formulations to describe the problem (Marinho, 2012; Silva & Marinho, 2016):

$$\nabla \cdot (r_\alpha \rho_\alpha \vec{U}_\alpha) = 0 \quad (5)$$

$$\begin{aligned} \nabla \cdot [r_\alpha (\vec{U}_\alpha \otimes \vec{U}_\alpha)] = \\ = -r_\alpha \nabla p + \nabla \cdot [r_\alpha (\tau_\alpha + \tau_\alpha^{turb})] + \vec{S}_{MS\alpha} + \vec{M}_\alpha \end{aligned} \quad (6)$$

The momentum balance on the right side of Equation 6 is a function of the pressure gradient ∇p , the shear stress τ_α , the external forces $\vec{S}_{MS\alpha}$, and the interfacial forces \vec{M}_α that act on phase α . The latter was considered as a function of the drag coefficient C_D , the mixture density $\rho_{\alpha\beta}$, and the interfacial area per unit volume $A_{\alpha\beta}$, as shown in Equation 7:

$$\vec{M}_\alpha = C_D \rho_{\alpha\beta} A_{\alpha\beta} |\vec{U}_\beta - \vec{U}_\alpha| (\vec{U}_\beta - \vec{U}_\alpha) \quad (7)$$

This study adopted $C_D = 0.44$ (the default value of Ansys CFX 13.0) in simulations. As for the convergence criterion, we used a root mean square (RMS) equal to 1E-6. Details regarding the mathematical modeling can be found in the **Ansys CFX 13.0's manual user (2011)** and **Marinho (2012)**.

2.5 Lockhart and Martinelli correlation

To predict the pressure gradient, we selected Lockhart and Martinelli correlation (Lockhart and Martinelli, 1949). It relies on the assumption that the two-phase pressure gradient is the product of the liquid pressure gradient by the two-phase frictional parameter ϕ_L^2 , as expressed in Equations 8, 9, and 10:

$$\left(\frac{dp}{dx}\right)_f^{TP} = \phi_L^2 \left(\frac{dp}{dx}\right)_f^L \quad (8)$$

$$\phi_L^2 = 1 + \frac{C}{X} + \frac{1}{X^2} \quad (9)$$

$$X^2 = \frac{\left(\frac{dp}{dx}\right)_f^L}{\left(\frac{dp}{dx}\right)_f^G} \quad (10)$$

The coefficient C (Equation 9) depends on the

Table 3. C values as a function of the idealized single-phased flow regimes.

Liquid phase flow regime	Gas phase flow regime	C
Laminar	Laminar	5
Turbulent	Laminar	10
Laminar	Turbulent	12
Turbulent	Turbulent	20

Source: Rahman et al., 2013.

idealized single-phased flow regimes of the liquid and the gas, and X^2 is the ratio of the single-phase pressure gradients (Equation 10). Table 3 shows the C values.

Equation 11 shows the appropriate Reynolds number used to determine the single-phased flow regime for phase α :

$$Re_{\alpha} = \frac{\rho_{\alpha} v_{\alpha} D}{\mu_{\alpha}} \quad (11)$$

Where v_{α} is the superficial velocity of the phase α . The single-phase pressure gradient for phase α was calculated using Equation 12:

$$\left(\frac{dp}{dx}\right)_{\alpha} = \frac{f_{\alpha} v_{\alpha}^2 \rho_{\alpha}}{2D} \quad (12)$$

The single-phased frictional factor f_{α} was determined using the Moody diagram with the Reynolds number of the phase.

2.6 Beggs and Brill correlation

We also used Beggs and Brill correlation for pressure gradient prediction due to its good agreement with experimental data, as reported in the literature (Sarah et al., 2014; Souza et al., 2010; Zhao et al., 2013). The total two-phased pressure gradient is composed of frictional, gravitational, and acceleration parcels, as shown in Equation 13.

$$\left(\frac{dp}{dx}\right)^{TP} = \left(\frac{dp}{dx}\right)_{f}^{TP} + \left(\frac{dp}{dx}\right)_{el}^{TP} + \left(\frac{dp}{dx}\right)_{acc}^{TP} \quad (13)$$

Where, subscripts f , el , and acc correspond to frictional, gravitational, and acceleration terms, respectively. In this study, we considered only the frictional term (Equation 14), for the pipe is horizontal and the fluids flow at a low velocity, in which the acceleration term is negligible. The frictional pressure gradient is a function of the two-

phase friction factor f_{TP} (Equation 15), which depends on the no-slip friction factor f_n . For the sake of simplicity, the full expression for the two-phase friction factor (Equation 15) was omitted in this work.

$$\left(\frac{dp}{dx}\right)_{f}^{TP} = \frac{f_{TP} \rho_n v_m^2}{2D} \quad (14)$$

$$f_{TP} = \theta(f_n) \quad (15)$$

The Moody diagram can be used to determine f_n for the Reynolds number expressed in Equation 16:

$$Re = \frac{\rho_n v_m D}{\mu_n} \quad (16)$$

Where ρ_n and μ_n represent the mixture's density and viscosity (Equations 17 and 18, respectively) weighted by the liquid input content λ_L (Equation 19):

$$\rho_n = \lambda_L \rho_L + (1 - \lambda_L) \rho_G \quad (17)$$

$$\mu_n = \lambda_L \mu_L + (1 - \lambda_L) \mu_G \quad (18)$$

$$\lambda_L = \frac{q_L}{q_L + q_G} \quad (19)$$

More details about the correlation can be obtained referring to Beggs and Brill (1991).

3. RESULTS AND DISCUSSION

This section compares the pressure gradients calculated from the three methods aforementioned: Ansys CFX, Lockhart and

Table 4. Mesh refinement test results.

Mesh	Number of elements	Pressure gradient (Pa/m) (Deviation (%) / CPU time (min))		
		Case 1 (bubbly flow)	Case 7 (plug flow)	Case 13 (stratified flow)
A	56,304	28,295 (- / 55)	7,341 (- / 57)	1,198 (- / 54)
B	109,417	30,357 (7.29 / 108)	6,782 (7.61 / 103)	1,093 (5.61 / 99)
C	224,961	31,084 (2.39 / 223)	6,698 (1.24 / 215)	1,108 (1.37 / 207)
D	325,149	30,295 (2.53 / 341)	6,753 (0.82 / 327)	1,067 (3.70 / 318)

Table 5. Heavy oil single-phased pressure gradients (Pa/m).

	$v_m = 0.8$ m/s	$v_m = 1.2$ m/s
Linear coefficient (Figure 4)	20,888	30,597
Equation 12	19,840	29,760
Percent relative deviation	5.28%	2.81%

Martinelli correlation, and Beggs and Brill correlation.

3.1 CFX results

To verify the accuracy of the numerical results, we performed a mesh refinement test with four meshes containing different numbers of elements. In this test, the pressure gradients of three cases (bubbly, plug, and stratified flow) were obtained using each mesh in the simulations, as shown in Table 4. To assess the influence of the number of elements on the pressure gradient, we calculated the percent deviation of mesh N considering the result of mesh $(N - 1)$ as reference (Equation 20). For example, the deviation for mesh C was calculated using the pressure gradient obtained in mesh B as reference.

$$Deviation_{mesh} (\%) = \left| \frac{\frac{dp}{dx_N} - \frac{dp}{dx_{N-1}}}{\frac{dp}{dx_{N-1}}} \right| \times 100\% \quad (20)$$

Table 4 shows that a finer mesh resulted in a more accurate solution. This is evidenced by the decrease in the deviation as the number of elements increased. For mesh B, the maximum deviation was 7.61 percent (case 7), which dropped

to less than 1 percent in mesh D. However, the CPU time, also computed in Table 5, increased considerably. The lowest time was 54 minutes for mesh A. On the other hand, the best simulation time was 6 times as high for mesh D. Adopting a tolerance of 10 percent in the deviation, one can observe that mesh B is suitable for this study due to its low CPU times and similar pressure gradients when compared to meshes C and D. For this reason, this mesh was used in all the numerical simulations.

After determining the optimum number of mesh elements, we analyzed the CFX results before comparing with the data of the correlations to verify if they qualitatively agree with the theory. Figure 4 shows the pressure gradient for the values of gas volume fraction, and mixture velocity presented in Table 2.

R^2 values show that pressure gradient decreases linearly with the increase of gas input content for both mixture velocities. One can also note that the pressure gradient was higher for $v_m = 1.2$ m/s since more energy is dissipated for a greater velocity. Although the oil single-phased flow was not simulated, the linear coefficients shown in Figure 4

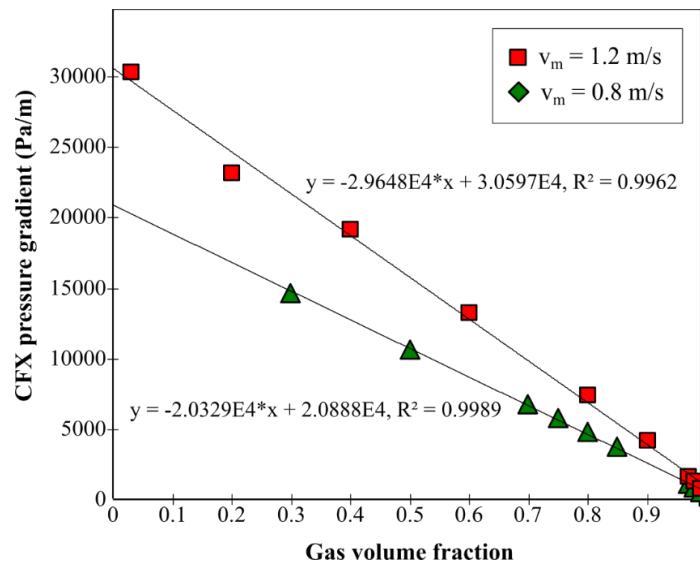


Figure 4. Influence of gas volume fraction and mixture velocity on pressure gradient.

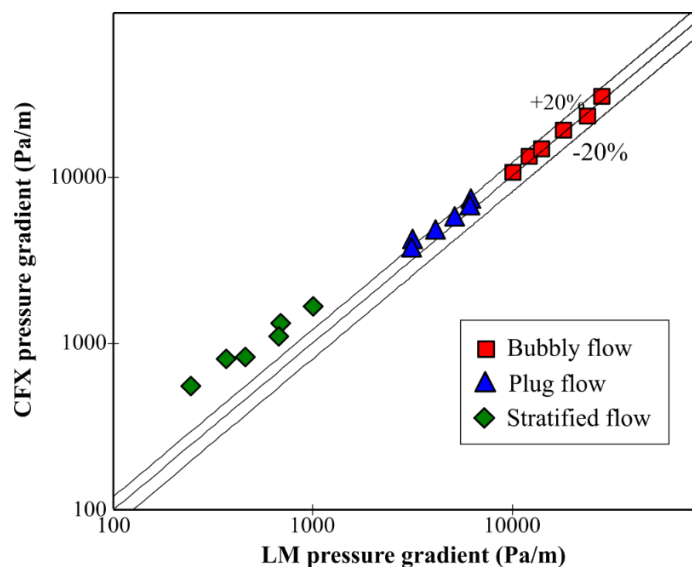


Figure 5. Comparison between the pressure gradients predicted by CFX and the Lockhart and Martinelli correlation.

agree with the single-phased pressure gradient predicted by Equation 12. The percent deviations between these values, with the results of Equation 12 used as reference, are computed in Table 5 for both mixture velocities.

The good agreement presented in Table 5 indicates that the heavy oil single-phased pressure gradient can be extrapolated from the graph in Figure 4.

3.2 Comparison with the correlation results

Since the CFX results exhibited a qualitative agreement with the theory presented, we can

move the discussion to the comparison with the pressure gradient predicted by the correlations. This is necessary because the results presented up to this point did not include the analysis about the influence of the flow pattern. The use of correlations for the following comparison is justified because of the lack of experimental data corresponding to physical conditions presented in this work. Figure 5 compares the CFX results with those of the Lockhart and Martinelli correlation.

Although non-drag forces such as lift, wall lubrication, and virtual mass forces were not considered in this work, the pressure gradients for bubbly and plug flows showed a good agreement with the correlation results, for which the

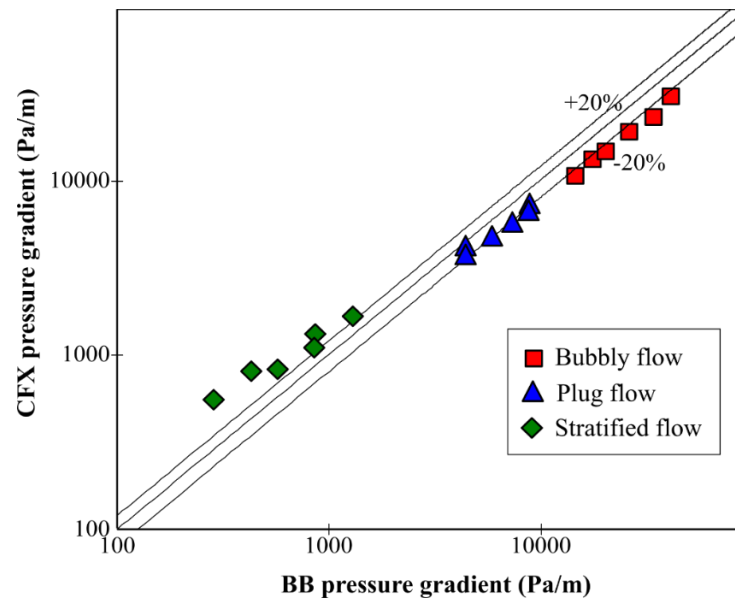


Figure 6. Comparison between the pressure gradients predicted by CFX and the Beggs and Brill correlation.

deviations are within 20 percent, as shown in Figure 5. Therefore, these forces are not relevant for these regimes under the conditions presented in this paper. However, the pressure gradients observed for stratified flow deviated more significantly from the correlation results (note the logarithmic scale of the axes). The pressure gradients predicted by Ansys CFX 13.0 are compared with those of Beggs and Brill correlation in Figure 6.

Beggs and Brill pressure gradients are higher than those predicted by the Lockhart and Martinelli correlation. According to Yuan and Zhou's study (2008), Beggs and Brill correlation over predicts the pressure gradient. The authors compared their results with experimental data and data from other correlations, which justifies the deviations over 20 percent obtained for bubbly and plug flows (Yuan and Zhou, 2008).

Figure 6 also shows that the stratified flow presented a poor agreement with the correlation results, as depicted in Figure 5. In both cases, the lack of agreement with this flow regime may be due to the instabilities that occur in the fluid's interface, since gas velocities are substantially greater than those of the oil. The modeling for stratified flow may require the use of turbulence as the gas velocity increases. For a better agreement, one can suggest the use of the Free Surface Model

since the interface is well defined in the flow pattern, and the calculation has different values for the drag coefficient, which depend on the velocity of the fluids but remained constant in this work for the sake of simplicity.

To analyze the influence of the gas input content even further, the percent deviation was calculated using Equation 21 for each case presented in Table 2. Figure 7 shows the percent deviation as a function of the gas volume fraction. Since the Beggs and Brill correlation over predicted the pressure gradient values, this analysis was performed for the Lockhart and Martinelli only.

$$Deviation_{CFX/LM} = \left| \frac{\frac{dp}{dx}_{CFX} - \frac{dp}{dx}_{LM}}{\frac{dp}{dx}_{LM}} \right| \times 100\% \quad (21)$$

The percent deviation for bubbly flow is lower than 10 percent in the worst case, indicating that the model proposed describes adequately this flow regime when comparing to the Lockhart and Martinelli correlation results. However, as the gas volume fraction increases, the percent deviation increases significantly for plug flow, and even more dramatically for stratified flow, reaching more than 100 percent. This result confirms the need of a more robust mathematical modeling to compute the effects of higher gas velocities. As

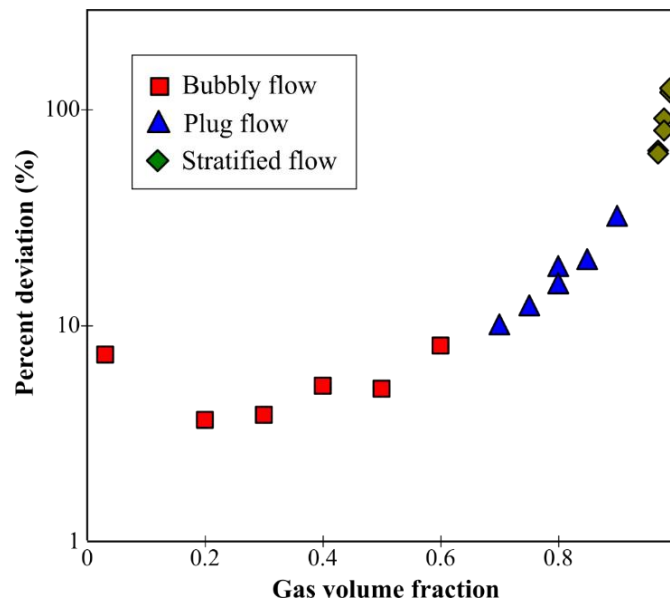


Figure 7. Percent deviation between CFX and the Lockhart and Martinelli correlation.

aforementioned, this may include turbulence and free surface models and adequate drag coefficient values.

To complete the analysis, the root-mean-square deviations (RMSD) between the pressure gradients for the numerical simulations and the Lockhart and Martinelli correlation were calculated using Equation 22. Table 6 shows these results:

$$RMSD = \left[\frac{1}{n} \sum_{i=1}^n (Deviation_{CFX/LM})^2 \right]^{0.5} \quad (22)$$

The RMS deviation for the bubbly flow was less than 6 percent when comparing the Ansys CFX and the Lockhart and Martinelli's results, demonstrating the good agreement between both methods for this flow regime. The pressure gradient for plug flow simulations deviated 19.55 percent from the correlation. As for the stratified flow, an RMSD percentage deviation greater than 90 percent was obtained, which is considerably high.

Table 6. RMSD between pressure gradients predicted by CFX and the Lockhart and Martinelli correlation.

Flow pattern	RMSD (%)
Bubbly	5.78
Plug	19.55
Stratified	93.58

4. CONCLUSIONS

In this communication, the authors presented a comparative study of the heavy oil and natural gas mixture pressure gradients for different flow patterns using the application Ansys CFX 13.0, and empirical correlations. The numerical results showed that the pressure gradient reduces linearly with the increase in the gas volume fraction, which agrees with the theory presented.

The Beggs and Brill correlation was found to over predict pressure gradients. Therefore, the correlation was not included in the statistical analysis. The observed pressure gradients for the bubbly and the plug flows obtained numerically presented a reasonable agreement with those predicted by the Lockhart and Martinelli correlation. The RMSD for bubbly flow was less than 6 percent using the results of the correlation as reference. The simulations for plug flow presented a deviation less than 20 percent, which can be considered acceptable.

Nevertheless, the numerical simulations for the stratified flow regime cases showed a poor agreement, with an RMSD greater than 90 percent. Turbulence and free surface models, as well as the use of different values of the drag coefficient, are suggested to improve agreement.

For future works, we suggest the use of other empirical correlations, or even experimental data if

available for a better analysis. As for the numerical simulations, we recommend a study in which the non-drag forces cannot be neglected. A new numerical model for stratified flows is recommended to consider the effects of a higher gas velocity.

ACKNOWLEDGEMENTS

We are grateful to the Laboratory of Separation Systems and Process Optimization (LASSOP/UFAL) for all the support provided during the training in Ansys ICEM CFD and Ansys CFX 13.0.

NOMENCLATURE

Latin letters:

$A_{\alpha\beta}$	Interfacial area per unit volume between phases α and β	m^{-1}
C_D	Drag coefficient	—
D	Pipe diameter	m
f_α	Friction fraction of phase α	—
f_n	No-slip friction factor	—
f_{TP}	Two-phase friction factor	—
g	Acceleration of gravity	m/s^2
m	Mass flow rate	kg/s
M_α	Interfacial forces on phase α	N/m^3
p	Pressure	Pa
r	Gas volume fraction	—
Re	Reynolds number	—
$S_{MS\alpha}$	External forces on phase α	N/m^3
U	Velocity vector	m/s
v_m	Mixture velocity	m/s

Greek letters:

α, β	Phases	—
ϑ	Angle with the horizontal plane	—
λ, ψ	Parameters of the Map of Baker	—
λ	Liquid input content	—
μ	Dynamic viscosity	$N.s/m^2$
ρ	Density	kg/m^3
σ	Surface tension	N/m
ϕ_L^2	Lockhart and Martinelli pressure gradient multiplier	—
τ^{turb}	Turbulent Reynolds stresses	$kg/(m.s^2)$

Symbols:

$\nabla \cdot$	Divergence operator	—
∇	Gradient operator	—
\otimes	Tensor product	—

5. REFERENCES

Angeli, P.; Hewitt, G. F. Flow structure in horizontal oil-water flow. **International Journal of Multiphase Flow**, p. 1117-1140, 2000.

[https://doi.org/10.1016/S0301-9322\(99\)00081-6](https://doi.org/10.1016/S0301-9322(99)00081-6)

ANSYS CFX 13. **User manual**. Ansys Europe Ltd., 2011.

Baker, O. Simultaneous flow of oil and gas. **Oil and Gas Journal**, p. 185-195, 1954.

Barbosa, L. M. C.; Lima, A. G. B.; Farias Neto, S. R. Non-isothermal Transient Three-Phase Flow (Heavy Oil, Water and Gas) in Vertical Pipeline: The Effect of Leakage. **International Journal of Modeling and Simulation for Petroleum Industry**, v. 6, p. 23-31. 2012.

Beggs, H. D.; Brill, J. P. **Two-phase Flow in Pipes**. 6th Edition. 1991.

Coates, J.; Pressburg, B. S. How to Analyse Two-Phase Flow. **Chemical Engineering**, 1959.

Foletti, C.; Farisè, S.; Grassi, B.; Strazza, D.; Lancini, M.; Poesio, P. Experimental investigation on two-phase air/high-viscosity-oil flow in a horizontal pipe. **Chemical Engineering Science**, p. 5968-5975, 2011.

<https://doi.org/10.1016/j.ces.2011.08.019>

Lockhart, R. W.; Martinelli, R. C. Proposed correlation of data for isothermal two-phase two-component flow in pipes. **Chemical Engineering Progress**, 1949.

Marinho, J. L. G. **Escoamento anular isotérmico de óleos pesados e água em bifurcações angulares: modelagem e simulação**. Tese de doutorado, Universidade Federal de Campina Grande, 2012. (in Portuguese)

Matsubara, H.; Naito, K. Effect of liquid viscosity on flow patterns of gas-liquid two-phase flow in a horizontal pipe. **International Journal of Multiphase Flow**, p. 1277-1281, 2011.

<https://doi.org/10.1016/j.ijmultiphaseflow.2011.08.001>

Sarah, A. A.; Julios, U. A.; Mary-Ann, O. Pressure Gradient Prediction of Multiphase Flow in Pipes. **British Journal of Applied Science & Technology**, v. 4, p. 4945-4958, 2014.

<https://doi.org/10.9734/BJAST/2014/12985>

Silva, L. D. S.; Marinho, J. L. G. Numerical Study on the Influence of Gas Volume Fraction on the Two-Phase Flow of Heavy Oil and Natural Gas Mixtures in an Oil Well. **Brazilian Journal of Petroleum and Gas**, v. 8, n. 2, p. 49-55, 2014.

<https://doi.org/10.5419/bjjpg2014-0004>

Silva, L. D. S.; Marinho, J. L. G. Study on Pressure Drop and Liquid Volume Fraction of The Oil-Gas Flow in a Vertical Pipe Using CFX and The Beggs And Brill Correlation: Viscosity Effects. **Brazilian Journal of Petroleum and Gas**, v. 10, n. 1, p. 001-008, 2016. <https://doi.org/10.5419/bjjpg2016-0001>

Souza, J. N. M.; Medeiros, J. L.; Costa, A. L. H.; Nunes, G. C. Modeling, Simulation and Optimization of Continuous Gas Lift Systems for Deepwater Offshore Petroleum Production. **Journal of Petroleum Science and Engineering**, v. 72, p. 277-289, 2010.

<https://doi.org/10.1016/j.petrol.2010.03.028>

Souza, J. S.; Farias, F. P. M.; Swarnakar, R.; Farias Neto, S. R.; Lima, A. G. B. Non-Isothermal Separation Process of Two-Phase Mixture Water/Ultra-Viscous Heavy Oil by Hydrocyclone. **Advances in Chemical Engineering and Science**, v. 1, p. 271-279, 2011.

<https://doi.org/10.4236/aces.2011.14038>

Thomas, J. E.; Triggia, A. A.; Correia, C. A.; Verotti Filho, C.; Xavier, J. A. D.; Machado, J. C. V. Souza Filho, J. E.; Paula, J. L.; Rossi, N. C. M.; Pitombo, N. E. S.; Gouvêa, P. C. V. M.; Carvalho, R. S.; Barragan, R. V. **Fundamentos de Engenharia de Petróleo**. 1. ed. Rio de Janeiro: Interciência: PETROBRAS, 2001. (in Portuguese)

Yuan, H.; Zhou, D. Evaluation of TwoPhase Flow Correlations and Mechanistic Models for Pipelines at Inclined Downward Flow. **Eastern Regional/AAPG Eastern Section Joint Meeting**. Society of Petroleum Engineering, 2008.

Zhao, Y.; Yeung, H.; Zorgani, E. E.; Archibong, A. E.; Lao, L. High viscosity effects on characteristics of oil and gas two-phase flow in horizontal pipes. **Chemical Engineering Science**, p. 343-352, 2013. <https://doi.org/10.1016/j.ces.2013.03.004>